



Serbian Tribology  
Society

# SERBIATRIB '09

11<sup>th</sup> International Conference on  
Tribology

Belgrade, Serbia, 13 - 15 May 2009



University of Belgrade  
Faculty of Mechanical  
Engineering

## TRIBOLOGICAL POTENCIAL OF ZINC-ALUMINIUM ALLOYS IMPROVEMENT

Babic Miroslav<sup>1</sup>, Mitrovic Slobodan<sup>1</sup>, Ninkovic Rato<sup>2</sup>

<sup>1</sup>Mechanical Engineering Faculty Kragujevac

<sup>2</sup>RAR d.o.o Batajnica

**Abstract:** In this paper are presented result of the study aimed at tribological improvement of ZA alloys. Two treatments of ZA-27 alloy were used: a) T4 heat treatment and b) reinforcement by graphite. The heat treatment of samples included the heating up to 370 °C for 3 or 5 hours, quenching in water and natural ageing. Graphite particles reinforced ZA-27 alloy composite materials were obtained by the compocasting procedure, which was executed by mixing at the isothermal regime (460 °C). Dry and lubricated sliding wear tests were conducted on as-cast and treated ZA-27 samples using block-on-disc machine over a wide range of applied loads and sliding speed. To determine the wear mechanisms, the worn surfaces of the samples were examined by scanning electron microscopy (SEM). The heat-treated alloy samples as well as reinforced samples attained significantly improved tribological behavior over the as-cast ones, both from the aspects of friction and wear.

**Keywords:** ZA27 alloy; Tribological behavior; Heat treatment; zinc-aluminum composites

### 1. INTRODUCTION

Commercially available ZA alloys (especially ZA27) have become the alternative material, primarily for aluminum cast alloys and bearing bronzes, due to good castability and unique combination of properties [1 - 12]. They can also be considered as competing materials for cast iron, plastics, and even for steels when being applied for operation under conditions of high mechanical loads and moderate sliding speeds (moderate operation temperatures) [6, 13, 14]. Interest for extending the practical application of these alloys is based on tribological, economical and ecological reasons. These alloys are relatively cheap and can be processed efficiently with low energy consumption, without endangering the environment [6, 15 - 17].

However, their broader application is limited. One of the major limitations of conventional zinc-aluminum alloys, containing 8 – 28 % Al, 1 – 3% Cu and 0.05% Mg (ZA8, ZA12 and ZA27), is the deterioration of their mechanical and wear resistance properties at elevated temperatures (above 100°C) and their dimensional instability [6, 13, 8 - 21]. Due to that, recent investigations have

focused attention to development of modified version of the ZA alloy.

The attempts have been made to partially replace copper by some high-melting element like Ni or Si and varying the quantity of aluminum up to 50% [2, 13, 22, 23, 24, 25]. In addition, heat treatment of ZA alloys is one of the possible measures for their improvement. The following procedures of heat treatment were used: a) artificial ageing of samples at temperatures from 90 to 150°C, mainly for optimizing the strength to specific elongation ratio [15, 21]; b) solutionizing (usually from 320 to 400°C) followed by artificial ageing (T6 type of heat treatment) [19, 20]; c) solutionizing with subsequent quenching and natural ageing (T4 type of heat treatment) [22, 26, 27]; d) solutionizing by rapid water quenching and ageing at elevated temperatures [23]; e) solutionizing followed by ageing at elevated temperatures and water quenching [24].

Heat treatment of the conventional zinc-aluminum alloys improves dimensional stability [15] and ductility [1, 20, 25]. However, the majority of the heat treatments lead to a reduction in hardness and tensile strength [19, 20, 26]. In

spite of reduced hardness, the heat-treated alloys attain improved tribological properties [19, 22, 23].

Good characteristics of ZA alloys have inspired researchers to reinforce them with different dispersed reinforcement materials (SiC, Al<sub>2</sub>O<sub>3</sub>, glass fibers, graphite and garnet) in order to obtain much more enhanced mechanical and tribological properties [14, 28 - 38]. As a result, in the recent years, MMCs based on ZA matrix are being increasingly applied as light-weight and wear-resistant materials.

Although the mentioned possibilities of ZA tribological characteristics improvement have been studied in the past there is still a lack of information. In view of the above, in this paper an attempt has been made to present and analyze the influence of heat treatment (T4 type of heat treatment) and reinforcement (by graphite) on microstructure, mechanical and wear behavior of ZA27 alloy.

## 2. EXPERIMENTAL PROCEDURE

### 2.1. Alloy preparation and characterization

ZA-27 alloy (27.6% Al, 2.5% Cu, 0.012% Mg and balance Zn) alloy was processed by the liquid metallurgy route. The ZA-27 alloy was processed by the liquid metallurgy route. The purity of aluminum was 99.90%, zinc 99.99 % and copper 99.5%. Alloy was melted in a graphite crucible in an electric resistance furnace. The melt was overheated to 680°C and cast into a steel mold to obtain samples as 100 mm long bars with rectangular cross-section with dimensions of 30 X 20 mm. Some of the alloy specimens were subjected to T4 heat treatment comprising solutionizing at 370°C for 3 h (ZA27 HT3), or 5 hours (ZA27 HT5), quenching in water and natural ageing at room temperature during more than 30 days.

The metal matrix composites with the ZA-27 substrate, reinforced by the graphite particles, were obtained by the compocasting procedure, which was executed by mixing at the isothermal regime (460°C). This procedure is characteristic by the fact that the reinforcers are being added during mixing the substrate in the semi solid state. The advantage of this procedure is that for its application, the reinforcer's particles do not have to be previously prepared, i.e., the procedure can be realized by particles, which do not have to be wetted in the metal solutions. The graphite particles of size 20 µm were added in the amounts of 1.5 mass %.

After obtaining the composite materials samples, it was necessary to perform the hot pressing to reduce porosity. The samples for the tribological investigations were then made from the

pressed pieces.

Microstructural characterization of the alloys was carried out using optical microscopy on samples similar to those used for wear testing. The specimens were polished according to standard metallographic practice and etched. Diluted nitric acid (5 vol%) in water was used as the etchant.

Bulk hardness of all samples was measured using a Brinell hardness tester with a 2.5 mm diameter steel ball indenter and under a load of 625 N. The load application time was 60 seconds. The prepared tensile samples had 4 mm gauge diameter and 20 mm gauge length. Tensile tests were conducted at ambient temperature (23°C) at a strain rate of 1.3x10<sup>-3</sup>/s using a universal testing machine. Reported data correspond to an average of five measurements.

### 2.2. Sliding wear tests

The specimens were tested using a computer aided block-on-disc sliding wear testing machine with the contact pair geometry in accordance with ASTM G 77 - 83. A schematic configuration of the test machine is shown in Fig. 1. The test block was loaded against the rotating steel disc. This provides a nominal line contact Hertzian geometry for the contact pair.

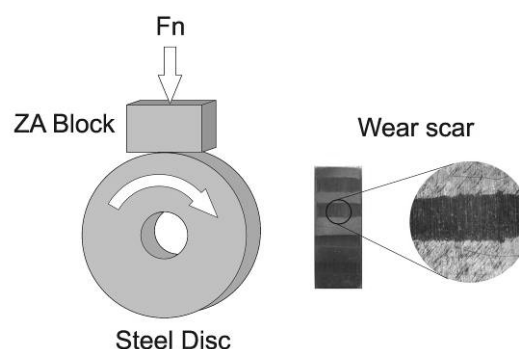


**Figure 1.** The scheme of contact pair geometry

The test blocks (6.35 x 15.75 x 10.16 mm) were prepared from the as-cast and heat-treated zinc-aluminum alloys. Their contact surfaces were polished to a roughness level of  $R_a = 0.2 \mu\text{m}$ . The counter face (disc with 35 mm diameter and 6.35 mm thickness) was fabricated using the casehardened 30CrNiMo8 steel with hardness of 55 HRC. The roughness of the ground contact surfaces was  $R_a = 0.3 \mu\text{m}$ .

The lubricated and dry tests were performed under applied loads of 10 – 100 N and sliding speeds of 0.26 – 1.0 m/s.

The lubricant used for the lubricated tests was ISO grade VG 46 hydraulic oil, a multipurpose lubricant, recommended for industrial use in plain and antifriction bearings, electric motor bearings,

machine tools, chains, and gear boxes, as well as in high-pressure hydraulic systems. During the lubricated tests, the discs were continuously

cast alloy (Fig. 2a and b) exhibited dendritic structure comprising primary  $\alpha$  dendrites surrounded by  $\alpha + \eta$  eutectoid and residual  $\eta$  phase

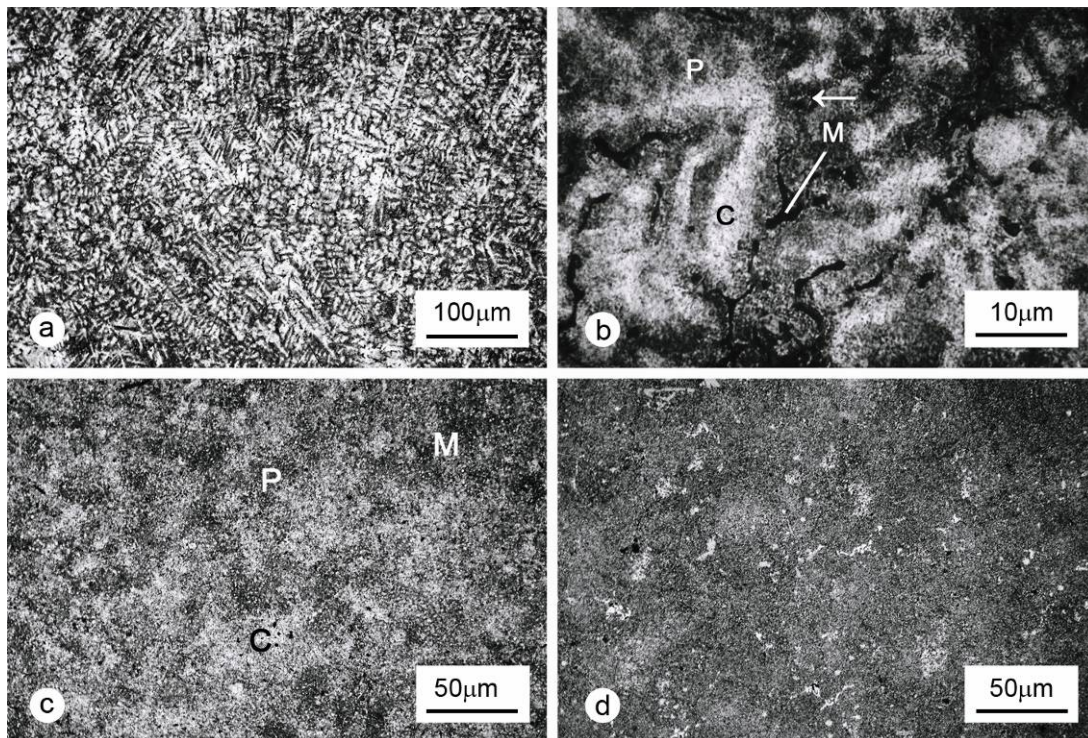


**Figure 2.** Microstructure of the alloy: (a and b) as-cast, (c) heat-treated with 3 h and (d) 5 h of solutionizing (C –  $\alpha$  dendrite core, P –  $\alpha + \eta$  dendrites' periphery, M –  $\eta$  interdendritic phase)

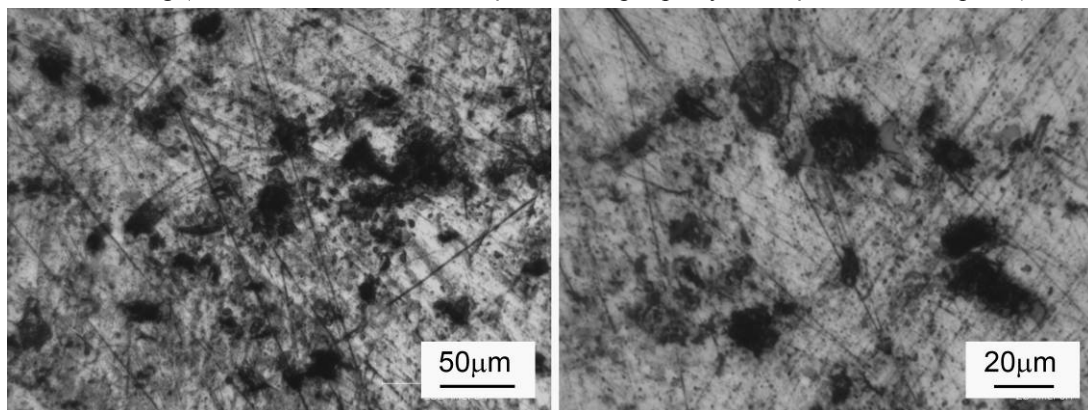


**Figure 3.** Optical micrograph of graphite particles reinforced ZA-27 alloy composite materials (polished surface)

immersed up to 3 mm of dept in 30 ml of lubricant.

The wear behavior of block was monitored in terms of the wear scar width. Using the wear scar width and geometry of the contact pair, the wear volume was calculated (Fig. 1). The SEM (“Philips XL30”) and OM (Meiji techno MT8500 Series) were used to examine the worn surfaces of the tested wear blocks. The friction coefficient was obtained automatically during the tests by means of the data acquisition software.

### 3. RESULTS

#### 3.1. Microstructure and mechanical properties

Microstructures of the alloys in as-cast and heat-treated conditions are presented in Fig. 2. The as-

cast alloy (Fig. 2a and b) exhibited dendritic structure comprising primary  $\alpha$  dendrites surrounded by  $\alpha + \eta$  eutectoid and residual  $\eta$  phase in the interdendritic regions. A magnified view of microstructure in Fig. 2b clearly shows these phases (marked by C –  $\alpha$  dendrite core, P –  $\alpha + \eta$  dendrites' periphery, M –  $\eta$  interdendritic phase).

With heat treatment, the micro-composition of ZA27 alloy became more homogeneous and the microstructure was refined (Fig. 2c and d). In the microstructure of ZA27 alloy, which was solutionized for 3 hours at 370°C and then quenched (Fig. 2c), one can distinct the residual dendrite cores and very fine  $\alpha + \eta$  mixture, which occupies the largest portion of the structure. After 5 hours of solutionizing, with consecutive quenching in water, the dissolution of the dendritic structure has occurred. Moreover, the uniformity of

distribution increased and size of various micro constituents decreased with the duration of solutionizing (Fig. 2d).

Fig. 3 (a and b) shows typical optical micrographs structures of the composite polished surface, which illustrated relatively uniform distribution of the graphite second phase. The graphite particles does not have sharp edges due to the collisions during the process of compocasting. Also, micrographs shows the pores which were left behind by evacuation of graphite particles from surfaces during polishing process.

**Table 1.** Mechanical properties of the alloys

| Alloys          | Treatment   | Tensile strength, MPa | Elongation, % | Hardness, HB |
|-----------------|---|-----------------------|---------------|--------------|
| ZA-27           | As-cast   | 318                   | 2.4           | 138          |
| ZA-27 HT3       | Solutionizing at 370°C for 3 h and quenching in water | 301                   | 5.2           | 121          |
| ZA-27 HT5       | Solutionizing at 370°C for 5 h and quenching in water | 283                   | 6.4           | 121          |
| ZA-27 composite | Graphite particle reinforced ZA-27                    |                       |               | 118          |

Mechanical properties of the tested samples are presented in Table 1. Heat treatment of the alloy caused a moderate decreasing of the tensile strength and hardness. Moreover, the heat-treated samples attained increased elongation as compared to that of the as-cast alloy. With regard to the solutionizing duration, it could be observed that it contributed to the tensile strength decrease and the elongation increase, while hardness became practically constant at longer solutionizing duration.

Presented results indicate hardness decreasing due to addition of graphite particles. It is in accordance with general fact that graphite reinforcement of Al and ZA alloys decrease hardness of material [26]. These effects increase with weight percent of graphite in composites.

### 3.2. Tribological behavior

#### a) Heat treated alloys

Based on wear scar width measurements, during the lubricated sliding process, the wear curves were plotted. Fig 4 illustrated on the example of wear curves obtained for ZA27 HT5 in all the combinations of applied loads and sliding speeds. By analyzing the shape of those curves, one concluded that the identical nature of the wear process development corresponded to all the tested materials, in all the contact conditions. Wear

behavior of tested alloys was characterized by the clearly expressed period of initial intensive wear (run-in) during the first minutes of sliding, after which the steady-state period follows. The steady-state wear is moderate and can be, with the high correlation coefficient, expressed as linear.

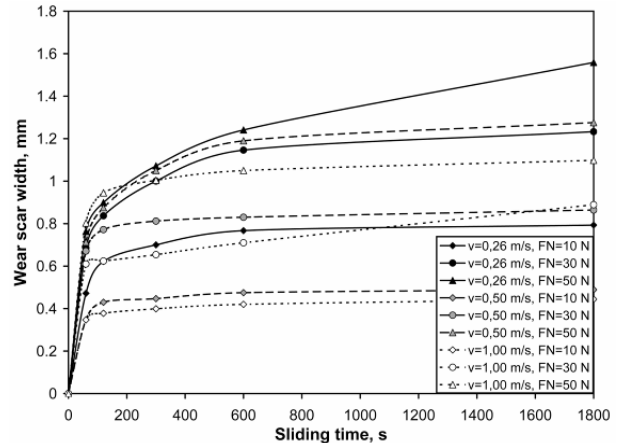


**Figure 4.** Wear curves of ZA27 HT5 alloy at different specific loads and sliding speeds (lubricated tests)

The character of friction coefficient variation during lubricated sliding is illustrated in Fig. 5. This is a graphical representation of the results obtained for ZA27 HT5 alloy with three levels of applied loads and two levels of sliding speed. From the diagram, one can clearly notice the run-in period, during which the intensive decrease of the friction coefficient occurs. During the steady-state period, the level of the friction coefficient is being stabilized. Such a dependence of the friction coefficient is in accordance with the described wear behavior of tested alloys.

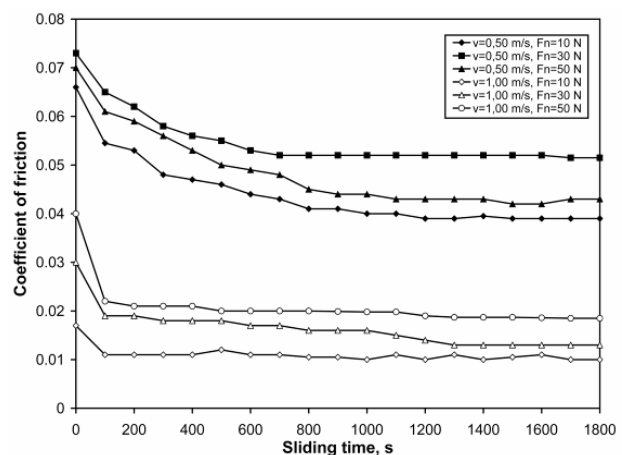


**Figure5.** Friction coefficient variation of ZA27 HT5 during sliding time at different specific loads and sliding speeds (lubricated tests)

Diagrams in Figure 6 show the dependence of the steady-state friction coefficient on the sliding speed, for various normal forces in conditions of lubricated sliding. The nature of that dependence, in

all the tested alloys, manifests as decrease of the friction coefficient with increase of the sliding speed. The degree of change is especially prominent in the region of lower values of speeds. Also, in all the tested alloys, the friction coefficient increases with increase of the normal force. The degree of increase is somewhat larger in the region of the lower normal loads (from 10 to 30 N).

In all the tested alloys, the friction coefficient decreases with increase of the  $v/F_n$  ratio. The graphical representation of the friction coefficient dependence on speed-to-load ratio,  $v/F_n$ , for the tested alloys is presented by the Stribeck curve in Figure 7. The graphs cover the boundary and the mixed lubrication regime. It confirms shape of the curves, as well as the obtained range of the friction coefficient (from 0.09 to 0.1). At the start of run, the lubricated system operates under boundary lubrication condition. However, as the sliding distance increases the thickness of the oil increases, giving rise to less metal-to-metal contact by producing mixed lubrication condition.

Based on the values of the wear scar width, the average values of the wear loss were calculated, expressed in  $mm^3$ . Diagrams in Fig. 8 present the dependence of the wear volume loss on the sliding speed for various normal forces in conditions of lubricated sliding. It can be seen that in all the alloys the wear volume decreases with increase of the sliding speed and decrease of the contact load. This is in accordance with the described lubrication conditions. The influence of the speed variation on wear is less expressed at lower sliding speeds.

The obtained results show existence of the significant differences in the friction and wear behavior of the tested alloys. It can be seen that the highest friction coefficient and volume wear loss, during the whole friction process, correspond to the as-cast alloys.

The average values of the friction coefficient for all the three levels of normal force and sliding speed are shown in Fig. 10. It can be noticed that for all the contact loads and sliding speeds the friction coefficient of heat-treated alloys is significantly reduced as compared to that of the as-cast one. Reduction rate is higher in area of lower applied loads.

These differences in the frictional behavior of the heat-treated alloys relative to the as-cast alloy versus speed-to-load ratio are also apparent in Figure 7. It can be seen that the Stribeck curves for the heat-treated alloys lie below and to the left with respect to the curve that corresponds to the as-cast alloy. This shows that higher loads and lower speeds can be tolerated by the heat-treated alloys.

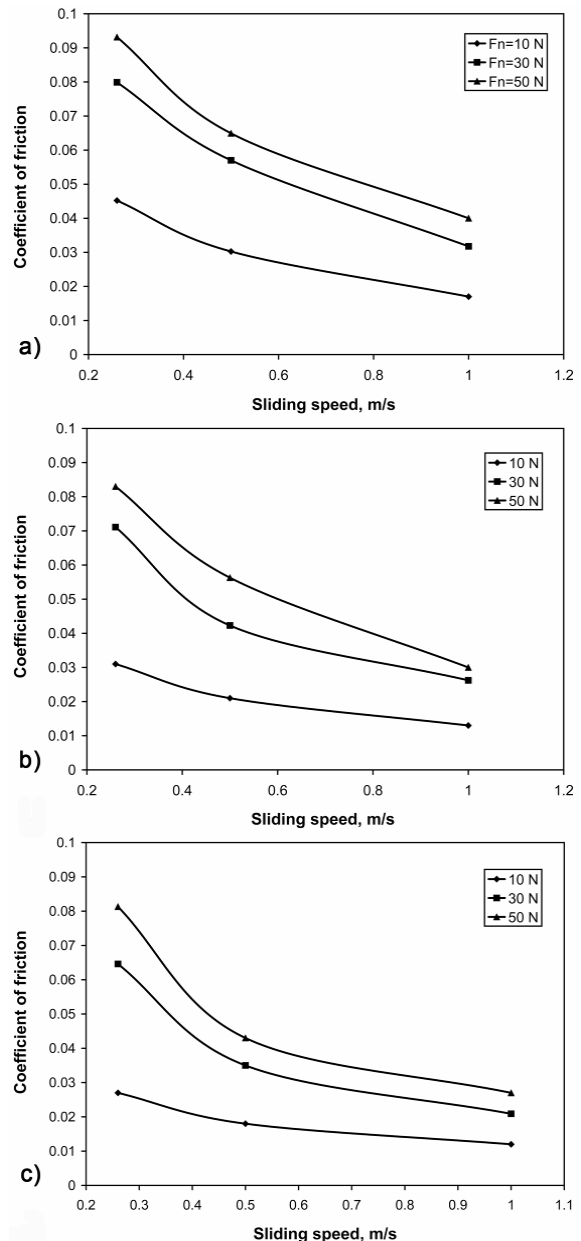


**Figure 6.** Friction coefficient vs. sliding speed for different applied loads: (a) ZA27 as-cast, (b) ZA27 HT3, (c) ZA27 HT5 (lubricated tests)

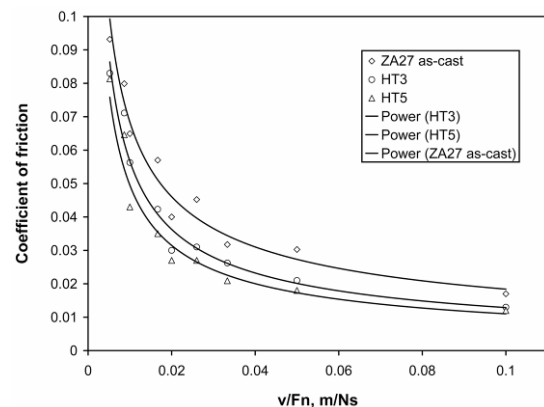


**Figure 7.** Friction coefficient of tested alloys vs. speed-to-load ratio (lubricated tests)

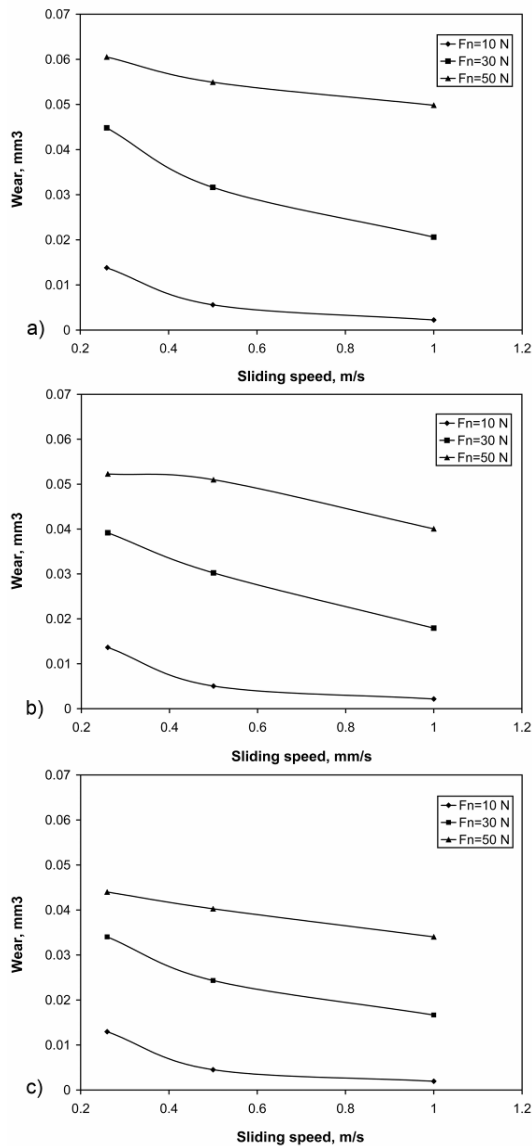


**Figure 8.** Wear loss of tested alloys vs. sliding speed for different applied loads: (a) ZA27 as-cast, (b) ZA27 HT3, (c) ZA27 HT5

The comparative wear losses of the tested alloys for all the three levels of normal force and sliding speed are shown in Fig. 10. The presented results clearly show that in the whole range of load and sliding speed, the wear loss of the heat-treated alloys is significantly lower as compared to that of the as-cast one. The decrease of the wear volume, expressed in percents, is somewhat more prominent at the highest contact load.

Characteristic features of the worn surfaces of tested alloys, obtained in condition of the highest applied load (50 N) and the lowest sliding speed (0.26 m/s) are shown in Fig. 11. Generally, the parallel grooves and scratches can be seen over all the surfaces in the direction of sliding (Fig. 11, marked by G). The wear surfaces of the heat-treated samples were noticed to be smoother than those of the as-cast one (Fig. 11b and c versus 11 a). A relatively clean surface marked by shallow grooves

(Fig. 11c and d) indicates the low wear loss. In contrast, significantly rougher worn surface with deep grooves, damages and smeared material (S) corresponds to the as-cast alloy (Fig. 11a and b).

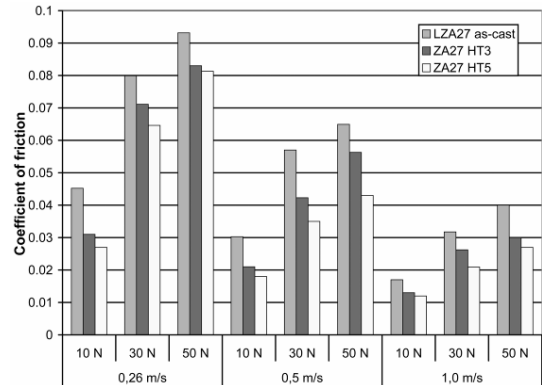


**Figure 9.** Friction coefficient of tested alloys comparison

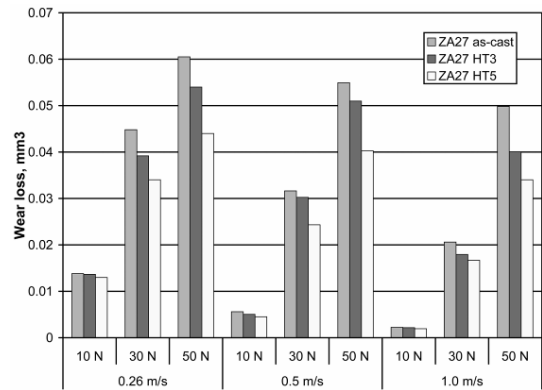


**Figure 10.** Wear volume loss of tested alloys comparison

The obtained results in dry tests show also existence of the significant differences in the friction behavior of the tested alloys. An example of those differences is presented in Fig. 12 for the case of friction at the lowest contact load of 15 N. It can be seen that the highest friction coefficient, during the whole friction process, corresponds to the as-cast alloy.

The average values of the friction coefficient for all four levels of normal force are shown in Fig. 13. In accordance with the nature of dry friction, the increase of the friction coefficient corresponds to the increase of the normal load. The increasing rate is especially evident for the load change from 15 to 30 N. It can be noticed that for all the contact loads the friction coefficient of heat-treated alloys is significantly reduced as compared to that of the as-cast one. The differences in the frictional behavior of heat-treated alloys relative to as-cast alloy decreases with the increase of load. The alloy solutionized for 5 h and quenched attained the lowest level of the friction coefficient for all tested loads.

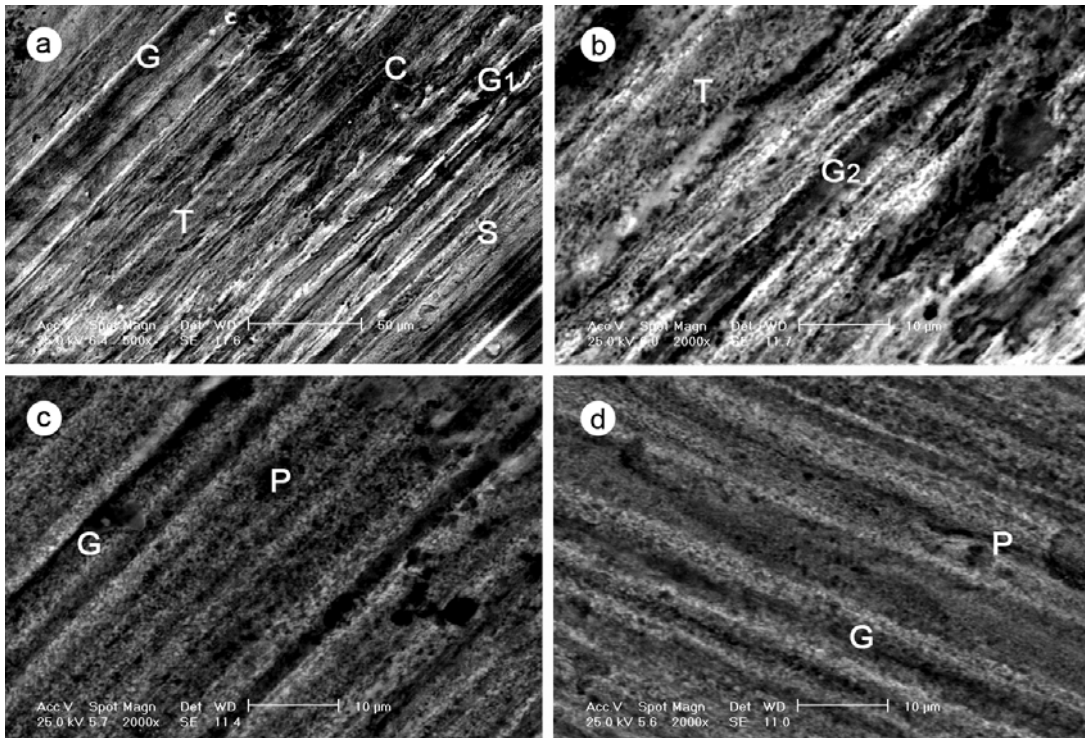


**Figure 11.** Wear surface of the alloys in lubricated sliding for 50 N of applied load and 0.26 m/s of sliding speed in conditions of lubricated sliding: a) ZA27 as-cast alloy, (b) ZA27 HT3 alloy, (c) ZA27 HT5 alloy

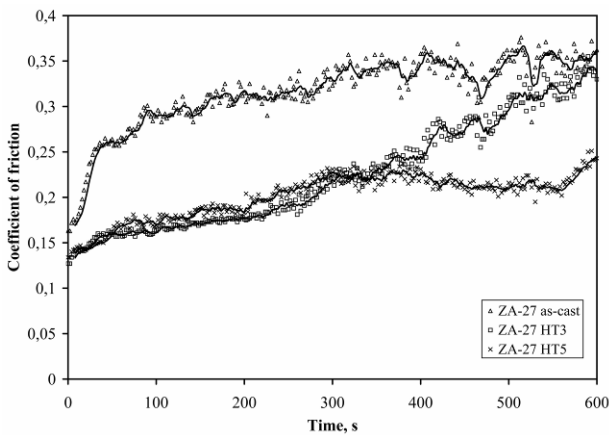


**Figure 12.** Coefficient of friction vs. sliding time curves for ZA-27 alloy in as-cast and heat-treated conditions (applied load 15 N, sliding speed 0.26 m/s) (dry sliding)

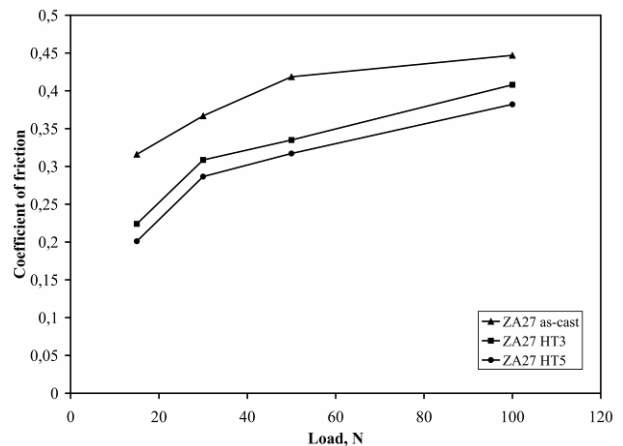


**Figure 13.** Coefficient of friction vs. applied load for ZA-27 alloy in as-cast and heat-treated conditions (dry sliding)

The comparative wear rate of the tested alloys as a function of the normal load is presented in Fig. 14. One can notice that for all the test alloys, the intensity of wear increases with the increase of the normal force. However, the gradient of that increase is not the same for all the alloys. The fastest increase corresponds to the cast alloy without the subsequent heat treatment. At the same time, for alloys that were heat-treated the gradient of change is significantly lower and approximately equal for both types of heat treatment.

The presented dependencies of the wear rate on the normal load clearly show that in the whole range of load, the wear rate of heat-treated alloys is significantly lower as compared to that of the as-cast one. This difference in their wear behavior is amplified in the area of higher loads, due to the mentioned higher influence of the normal load increase on the wear rate increase for the as-cast alloy. The lowest wear rate corresponds to the alloy annealed for 5 hours, quenched in water.

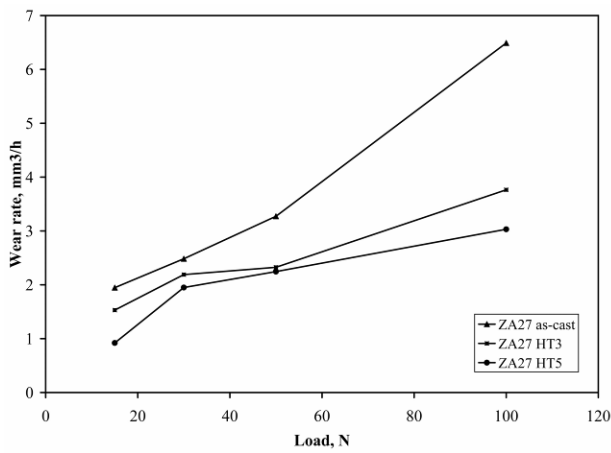


**Figure 14.** Wear rate vs. applied load for ZA-27 alloy in as-cast and heat-treated conditions (dry sliding)

gets entrapped in between the contacting surfaces and behaves as a cutting tool causing abrasion [20, 24].

Besides abrasive wear mechanism, existence of the material smeared onto the sliding surface (clearly visible in Fig. 15a and b, marked by B) shows presence of the adhesive wear. This material had been detached from the alloy surface by adhesion to the steel surface [25]. During sliding, some of transferred material was lost, but some re-embedded and was smeared over the alloy sample surface.

In addition, scanning electron micrograph shown in Fig. 15 exhibits the typical appearance of the surface fatigue damages after repeated unidirectional sliding of block over disc. The forms

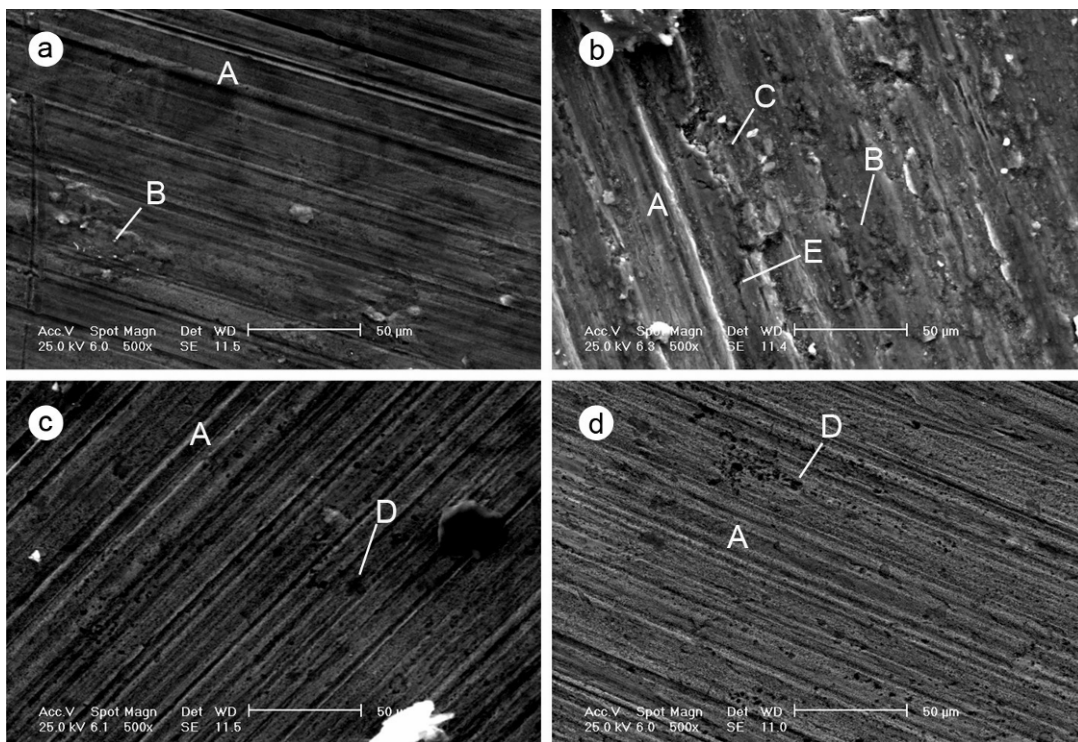


**Figure 15.** Wear surfaces of the ZA-27 alloy in as-cast conditions for applied load of 15 N (a) and 50 N (b) and after heat treatment for applied load of 50 N: (c) ZA-27 HT3 and (d) ZA-27 HT5 (A - ploughing grooves B- smeared material, C - spalls, D - pits, E - surface cracks) (dry sliding)

The worn surfaces of the samples are shown in Fig. 15. The worn surfaces of the heat-treated samples were noticed to be smoother than those of the as-cast one (Fig. 15c and d versus 15b). Generally, the parallel ploughing grooves and scratches can be seen over all the surfaces in the direction of sliding (Fig. 15, marked by A). These grooves and scratches resulted from the ploughing action of asperities on the counter disc of significantly higher hardness. Simultaneously with this two-body abrasive wear, the three-body abrasive wear takes place, due to the abrasive action of the hard wear debris emanating from fragmented and oxidized asperities of alloy and abraded surface of steel disc [24]. Such hard debris

of surface fatigue damage are spalls (craters of different depths and shapes on contact surface marked by C), pits (marked by D) and surface cracks (marked by E). The SEM examination of the subsurface regions (below the wear surfaces) in similar study on the same alloy [20] clearly demonstrated appearance of micro constituents flow in sliding direction and subsurface cracks. These subsurface cracks nucleated due to the stresses propagate during the sliding process. When such subsurface cracks join the wear surface, delamination of material occurs. This mechanism of wear is described by delamination theory of wear, introduced by Suh [39]. Contact surfaces of ZA-27 alloy are not subjected to fatigue failures only as a

result of repeated stressing caused by moving asperities of steel disc. Hard wear debris trapped by the two moving surfaces during dry sliding could have significant role in fatigue wear particles forming [40].

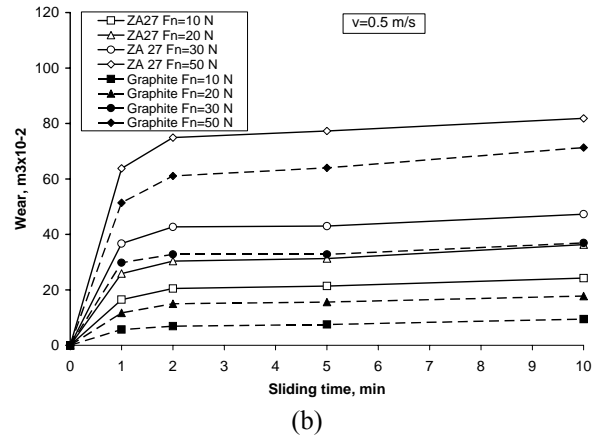
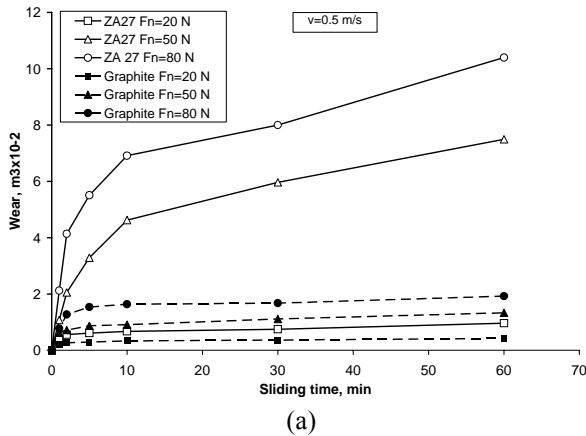


**Figure 16.** Wear curves of tested samples in conditions of lubricated (a) and dry sliding conditions (b)

b) ZA-27/graphite composite

Wear behavior of tested ZA-27/graphite composite samples in lubricated and dry sliding conditions is illustrated in Fig 16 (a and b) on the example of wear curves obtained in tests with 0.5 m/s of sliding speed for varying applied loads. Generally, wear behavior of tested materials is characterized by the clearly expressed period of initial very intensive wear (run-in) during the first minutes of siding, after which the steady-state period follows.

It could be noticed that wear of the composites with addition of the graphite particles is always significantly lower compare to the matrix ZA-27 alloy

Fig. 17 (a and b) show the wear volume loss of the all tested materials as a function of applied pressure at different sliding speeds in conditions lubricated sliding (Fig. 17a) and in conditions dry sliding (Fig. 17b). These plots indicate that wear volume loss of the matrix alloy as well as the composite increase with applied load at tested sliding speeds (0.26, 0.5 and 1.0 m/s).

The effect of sliding speed on wear volume loss of composite as well as the base alloy specimens at applied loads (10, 30 and 50 N - for lubricated sliding, and 30, 50 and 80 N – for dry sliding) is presented in Fig. 18. Nature of sliding speed influence onto wear is different for lubricated and dry wear tests. In the first case the wear volume loss of both the unreinforced alloy as well as composite specimens increases with increase in the sliding velocity. On the contrary, in conditions of lubricated sliding increase of sliding speed effects decrease of wear volume loss.

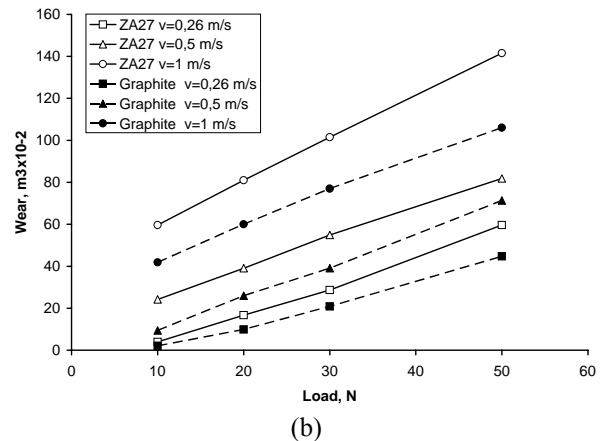
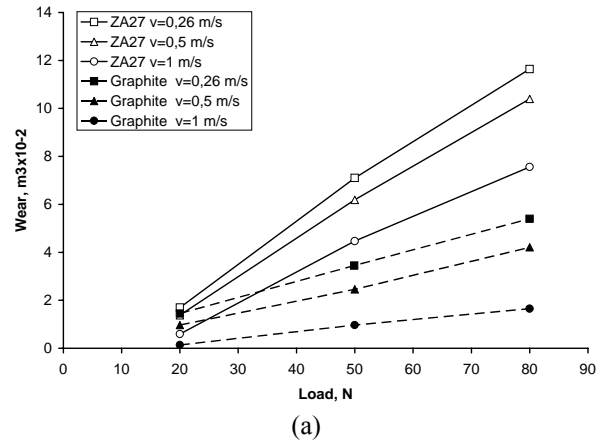


**Figure 17.** Wear volume vs. applied load: (a) lubricated sliding, (b) dry sliding

In conditions of dry sliding the wear behavior of test materials differs more significantly at higher sliding speed and higher normal load. At the same time, tribological behavior differences of tested materials increase with sliding speed decreasing and applied load increasing in conditions of lubricated sliding..

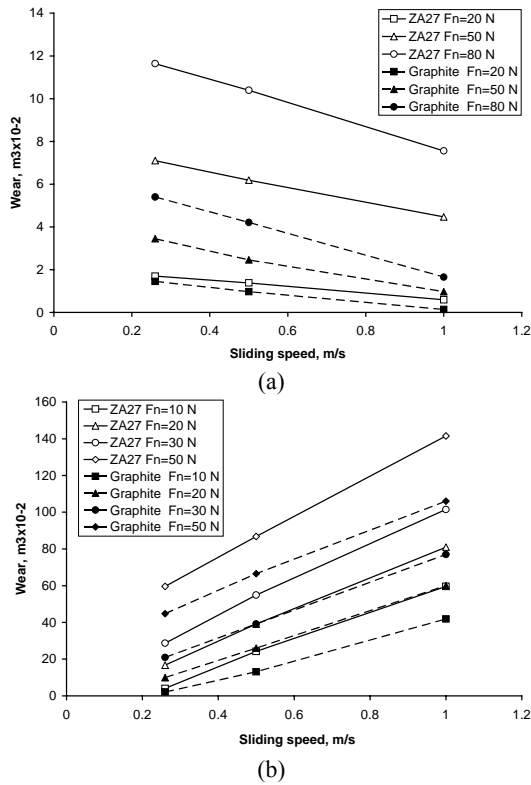


**Figure 18.** Wear volume vs. sliding speed: (a) lubricated sliding, (b) dry sliding

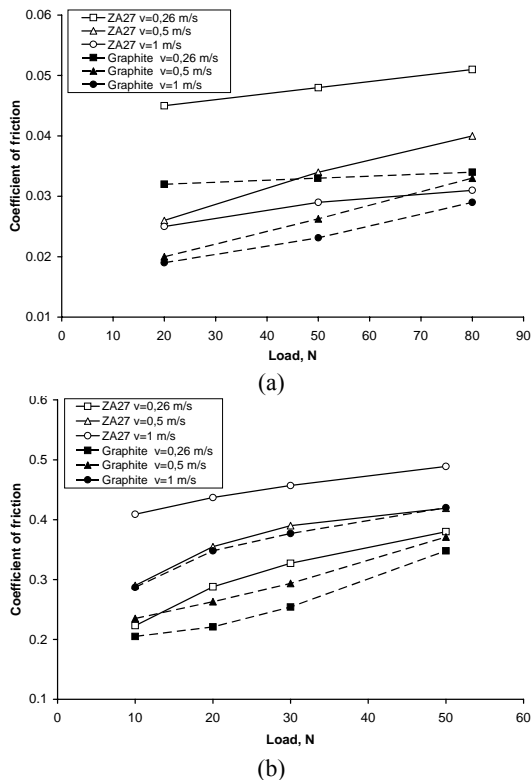


**Figure 19.** Coefficient of friction vs. applied load: (a) lubricated sliding, (b) dry sliding

Figure 19 shows the steady-state friction coefficient of the tested materials as a function of applied load at different sliding speeds in lubricated (Fig. 19a) and dry conditions (Fig. 19b). These plots indicate that friction coefficient of the matrix

alloy as well as the composite increase with applied load at tested sliding speeds (0.26, 0.5 and 1.0 m/s).

Diagrams in Figure 20 show the dependence of the steady-state friction coefficient on the sliding speed, for various normal forces. The nature of that dependence in lubricated conditions manifests as decrease of the friction coefficient with increase of the sliding speed (Fig. 20b). On contrary, in conditions of dry sliding coefficient of friction increases with sliding (Fig. 20a).

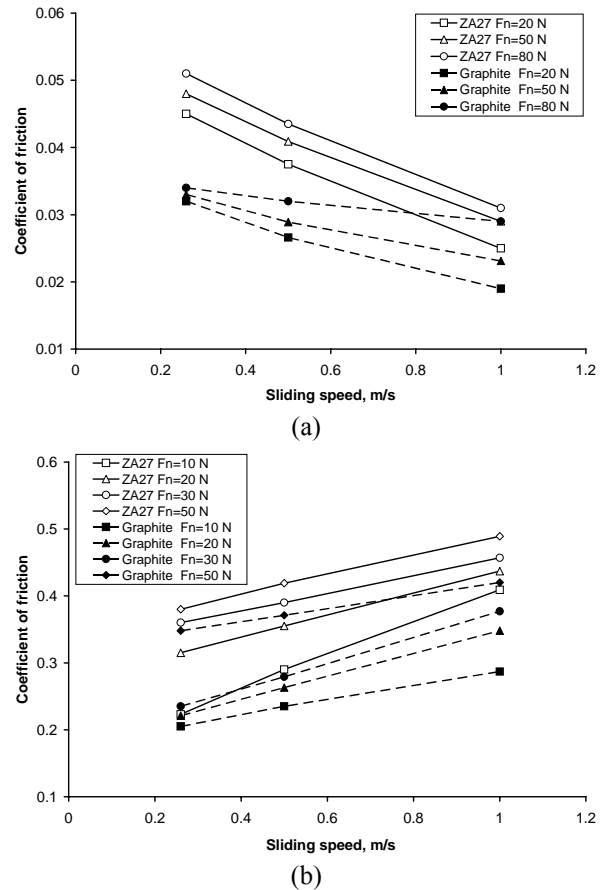


**Figure 20.** Coefficient of friction vs. sliding speed: (a) lubricated sliding, (b) dry sliding

Generally, it can be seen that the highest friction coefficient, during the whole friction process, corresponds to the composite material.

The worn surfaces of the samples, obtained in test with the highest applied load of 50 N and sliding speed of 1.0 m/s, are shown in Fig. 21. The worn surfaces of the composite samples were noticed to be much smoother than those of the as-cast alloy (Fig. 22b versus 22a). The appearance of deep grooves along with surface cracks at worn surfaces of alloy shows that intensive abrasive and fatigue wear took place. In contrast, the worn surfaces of composite are characterized by shallow grooves in direction of sliding and smeared graphite all over wear scar (Fig. 22b).

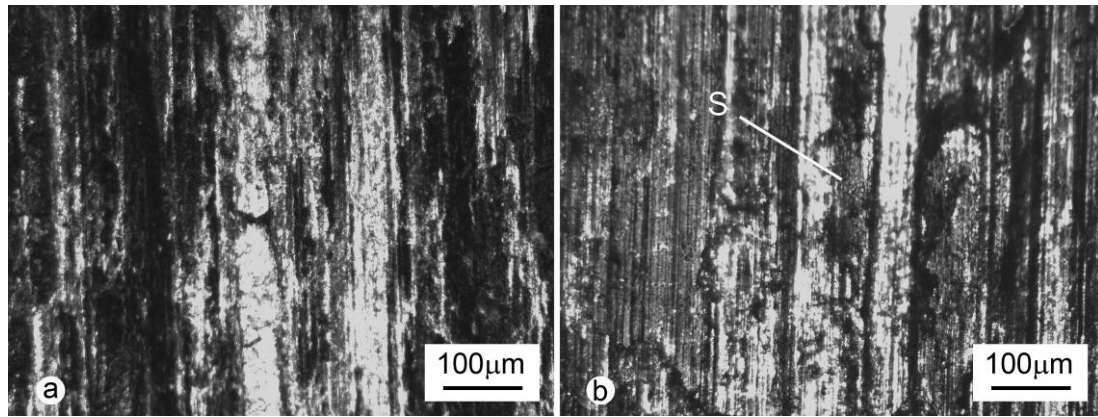


**Figure 21.** Worn surfaces in conditions of dry sliding with 50 N of applied load and 1.0 m/s of sliding speed: (a) ZA-27, (b) Graphite particles reinforced ZA-27 alloy composite

#### 4. DISCUSSION

The hardness and tensile strength of the heat-treated samples decreased while their elongation increased as compared to that of the as-cast alloy (Table 1). The softening rate of the alloy (12.4%) is practically constant with solutionizing duration. On the contrary, increasing of the solutionizing duration caused the strength to decrease and elongation to increase.

In spite of reduced hardness, the friction coefficient and wear volume loss of heat-treated alloy samples were significantly lower than that of as-cast alloy samples (Figs. 9 and 10). The positive effects of the heat treatment on the zinc-aluminum alloys in spite of reduction in hardness and strength have been suggested also by Prasad [19, 20, 24].

The explanation for the obtained results should be looked for in heat treatment effects on the microstructure of alloy. The influence of the microstructure on tribological behavior of samples can be manifested directly and indirectly. The former one refers to the direct influence of the microstructural characteristics on the tribological behavior of an alloy. The latter one is manifested via the residual stresses influence on micro scale and ductility of alloy in contact layers, which can be directly related to the established wear mechanisms of samples.

The dendritic microstructure of the as-cast alloy was characterized by the non-uniform distribution of micro constituents. The heat treatment has, by diffusion, dissolved the non-equilibrium dendritic structure, and contributed to high increased share of the two-phased  $\alpha + \eta$  mixture in the final material structure.

The  $\alpha$ -Al rich solid solution provides strengthening and thermal stability to alloys in view of the higher melting point of Al (than that of Zn). In addition, this phase with face-centered cubic crystal structure (f.c.c.) is characterized by good

work hardening capability, that contributes to wear behavior improvement of the alloys [2, 26]. The  $\eta$ -Zn rich solid solution has a hexagonal-close-packed crystal structure (h.c.p.) with a higher  $c/a$  ratio than observed in ideally close packed hexagonal crystal system [2]. Thanks to that characteristic, the  $\eta$  micro constituent has very good smearing characteristics, acting as a solid lubricant. Moreover, the  $\eta$  phase also acts as a load-bearing phase because of its hexagonal structure [2, 3]. Effects of these micro constituents on tribological behavior of the alloy depend on their distribution, size, and operating temperatures.

Just the finer and well-distributed micro constituents (hard and soft phases), achieved by heat treatment (Fig. 2 c and d), contributed to reducing the friction and wear. There, self-lubricating role of  $\eta$  micro constituent is especially precious in dry sliding, as well as during the running-in process of lubricated sliding, which is characterized by the boundary lubrication and intensive wear.

Besides that, the changes of microstructure due to heat treatment are significant, on a micro-scale, from the aspect of residual stresses, which affect the wear mechanism. The dendritic non-homogeneous structure of as-cast alloy is characterized by presence of residual stresses on a micro-scale, which appear due to different thermal characteristics and mechanical properties of various phases [20]. Improvement of uniformity, due to the heat treatment, relieved the residual stresses, as is also evident from decreasing of hardness and strength and increasing of elongation (Table 1) after the heat treatment [20, 25].

The described influence of heat treatment on improvement of tribological behavior of ZA27 alloy is in accordance with morphology of the worn surfaces that are presented in Figs. 11 and 15.

The worn surface of the as-cast alloy in conditions of lubricated sliding is characterized by

deep continuous grooves (Fig. 11 marked by G, G<sub>1</sub>, G<sub>2</sub>), scratches (S), pits/craters (C/P) and smeared material (T). These grooves and scratches resulted from the ploughing action of asperities on the counter disc of significantly higher hardness, as well as due to the hard wear debris, emanating from fragmented and oxidized asperities of alloy and abraded surface of the steel disc [25]. On the worn surface of the as-cast alloy different types of grooves could be clearly noticed. Only the rare grooves fit right into the material model removal and displacement in ductile abrasive wear (Fig. 11a marked with G). In this model, during abrasive wear the material does not simply disappear from the groove gouged in the surface by a micro abrasive element. Instead, a large proportion of the gouged or abraded material is envisaged as being displaced to the sides of the micro abrasive element path [29]. The dominant groove morphology points to the non-ductile abrasive wear. That was proved by the wear grooves characterized by micro cracks appearance in material displaced to the sides of grooves (Fig. 11a marked with G<sub>1</sub>). During the friction process, this material was removed as a product of wear, because of propagating micro cracks. In addition, the grooves with material spalled at the sides of grooves are present on the worn surface (Fig. 11b marked with G<sub>2</sub>).

Besides the abrasive wear mechanism, existence of the material smeared onto the sliding surface (clearly visible in Fig. 11a and b, marked by T), shows presence of the adhesive wear. This material had been detached from the alloy surface by adhesion to the steel surface [25]. During the sliding, some of transferred material was lost, but some was re-embedded and was smeared over the alloy sample surface. In addition, the scanning electron micrograph shown in Fig. 11, exhibits moderate appearance of the surface fatigue damages after repeated unidirectional sliding of block over the disc (C).

The rough worn surface with deep grooves, damages and smeared material corresponds to the as-cast alloy (Fig. 15b) in conditions dry sliding. It is a consequence of intensive abrasive and adhesive wear. The phenomenon of delamination also contributes to higher wear of the as-cast alloy with respect to the heat-treated one, what can be approved by the surface fatigue damages (Fig. 15b, marked by C). The prominent delamination wear of the as-cast alloy could be explained by residual stresses on a micro-scale, resulted from non-uniform distribution of various micro constituents. This wear mechanism of as-cast alloy was noted for wear tests in conditions of higher loads (Fig. 15b versus a).

Characteristics of wear surfaces are in accordance with determined effects of applied load on wear response of tested alloys, shown in Fig. 6. The data plots show considerable higher slope of line corresponding to as-cast alloy compared to heat-treated alloys. Slope increase can be clearly noticed at the applied load change from 30 to 50 N, and it is especially prominent at the further increase of the applied load up to 100 N. This difference in wear degree increase with load of as-cast alloy, with respect to heat treated alloys, is a consequence of the described phenomenon of delamination as a dominant mechanism, which occurs in the area of higher applied loads.

The worn surfaces of heat-treated alloys shown in Fig.11 (c and d) and 15 (c and d) are relatively smooth with shallow wear grooves, resulted from mild abrasive wear. Also, no smearing was observed on the worn surfaces. Unlike the worn surface of the as-cast alloy, the wear grooves on surfaces of heat-treated surfaces are abraded in accordance with model of ductile abrasive wear (Fig. 11c and d, marked with G). That type of abrasive wear is influenced increased ductility because of heat treatment (Table 1).

The positive effects of heat treatments on tribological behavior of alloy are slightly higher for longer time of solutionizing. This is also conformed by the SEM micrographs in Fig. 11c and d. It is in accordance with higher the uniformity of distribution and decreased size of various micro constituents and increased ductility.

The graphite particle reinforcing influenced significant tribological improvement of ZA-27 matrix material. This improvement could be explained by triboinfluenced graphite film formation and its effect on friction and friction reduction [14].

Self-lubricating role of graphite in sliding contact is provided by layered-lattice structure. Namely, graphite is characterized by hexagonal layered structure. The bonds between the parallel layers are relative weak (van der Waals type). Except that, graphite reacts with gases (such as water vapor) forming strong chemical bonds. The adsorbed water vapor and other gases from environment onto the crystalline edges weaken the interlayer bonding forces. It results in easy shear and transfer of the crystalline platelets on the mating surfaces.

The self-lubricated role of graphite reinforcing particles were significant in dry sliding conditions, as well as in conditions of lubricated sliding.

The free graphite particles released from the composite material during dry sliding of mating surfaces form a lubricant film at the interface

(‘third body’). On that way solid-solid interactions modifies to solid-lubricant-solid inreactions.

In conditions of lubricated sliding the positive tribological effects of graphite can be attributed to the its influence on tribological characteristics of lubricating oil. Namely, powdered solid lubricants (as graphite, MoS<sub>2</sub> and PTFE) as additive to lubricants are commonly used for variety industrial applications. In the present case, the released graphite shears into very fine particles under applied load and forms oil-graphite emulsion, which smears over the entire mating surface forming an effective layer of lubricant [37].

The described effect of graphite confirm the micrographs of worn surfaces. The micrographs presented in Fig. 21 show the worn surfaces of matrix alloy and composite obtained in conditions of dry friction and applied load of 50 N. The alloy surface shows extensive surface ploughing along with local delimitation and highly damages. The composite surface is not much damaged, bat has continues shallow grooves. Also, the presence of smeared graphite can be seen (the dark spot shown in Fig. 21b, marked by S). The graphite, as a soft second phase, has been squeezed out from subsurface toward the mating surface due to plastic deformation.

## 5. CONCLUSIONS

The heat-treated alloy samples attained improved tribological behavior (reduced coefficient of friction and wear rate) over as-cast ones, for all applied loads in lubricated and dry sliding conditions. The improved tribological behavior of the heat-treated alloys, in spite of reduced hardness, could be attributed to finer and more uniform distributed micro constituents and reduced cracking tendency.

Dominant wear mechanisms for tested alloys were abrasion and adhesion. However, under conditions of higher applied load delamination has considerable role in wear process of as-cast alloy. Due to that, difference in wear behavior of heat-treated versus as-cast alloy is amplified in the area of higher loads. The worn surfaces morphologies of heat-treated alloys pointed out more ductile mode of fracture than the as-cast alloy.

The graphite particle reinforcing influenced significant tribological improvement of ZA-27 matrix material. This improvement in conditions of dry sliding could be explained by triboinfluenced graphite film formation and its effect on friction and friction reduction. In conditions of lubricated sliding the positive tribological effects of graphite can be attributed to the its influence on tribological characteristics of lubricating oil.

## REFERENCES

- [1] J. P. Pandey, B. K. Prasad, A. H. Yegneswaran: *Dry sliding wear behavior of a zinc-based alloy: a comparative study with a leaded-tin bronze*, Materials Transactions (JIM) 39, 1121–1125, 1998.
- [2] M. T. Abou El-khair, A. Daoud, A. Ismail: *Effect of different Al contents on the microstructure, tensile and wear properties of Zn-based alloy*, Materials Letters 58, 1754–1760, 2004.
- [3] T. Savaskan, S. Murphy: *Comparative wear behavior of Zn-Al based alloys in an automotive engine application*, Wear 98, 151-161, 1984.
- [4] T. S. Calayag: *The practicality of using Zinc-Aluminum alloys for friction-type bearings*, Proc. of 25th Annual Conference of Metallurgists, pp. 305-313, 1986.
- [5] T. Savaskan, S. Murphy: *Mechanical properties and lubricated wear of Zn-Al based alloys*, Wear 116, 211-224, 1987.
- [6] E. J. Kubel: *Expanding horizons for ZA alloys*, Advanced materials & processes inc. Metal Progress 7, 51-57, 1987.
- [7] F. Goodwin, A. Ponikvar: *Engineering properties of zinc alloys*, Third edition, ILZRO, 1989.
- [8] R. J. Barnhurst: *Designing Zinc Alloy Bearings*, J. Materials Engineering 12, 279-285, 1990.
- [9] J. P. Pandey, B. K. Prasad: *Sliding wear response of a zinc-based alloy compared to a copper-based alloy*, Metallurgical and materials transactions 29, 1245-1255, 1989.
- [10] A. Rac, M. Babić, R. Ninković: *Theory and practice of Zn-Al sliding bearings*, Journal of the Balkan Tribological Association 7, 234-240, 2001.
- [11] M. Babic, R. Ninkovic: *Zn-Al alloys as tribomaterials*, Tribology in industry 26, 3-7, 2004.
- [12] M. Babic, R. Ninkovic, A. Rac: *Sliding wear behavior of Zn-Al alloys in conditions of boundary lubrication*, The Annals of University “Dunărea De Jos “ of Galați Fascicle VIII, Tribology, 60–64, 2005.
- [13] P. Choudhury, S. Das, B. K. Datta: *Effect of Ni on the wear behavior of a zinc-aluminum alloy*, Journal of materials science 37, 2103–2107, 2002.
- [14] S. C. Sharma, B. M. Girish, R. Kamath, B. M. Satish: *Graphite particles reinforced ZA-27 alloy composite materials for journal bearing application*, Wear 219, 162–168, 1998.
- [15] E. Gervais, R. J. Barnhurst, C. A. Loong: *An analysis of selected properties of ZA alloys*, Journal of metals 37, 43-47, 1985.
- [16] Y. H. Zhu, Y. Biao, H. Wei: *Bearing wear resistance of monotectoid Zn-Al based alloy (ZA-35)*, J. Mater. Sci. Technol. 11, 109-113, 1995.
- [17] R. Lyon: *High strength zinc alloys for reengineering applications in the motor car*, Metals and materials 1, 55–57, 1985.

- [18] I. Bobic, R. Ninkovic, M. Babic: *Structural and mechanical characteristics of composites with base matrix of RAR27 alloy reinforced With Al<sub>2</sub>O<sub>3</sub> and SiC particles*, Tribology in industry 26, 21–26, 2004.
- [19] B. K. Prasad, A. K. Patwardhan, A. H. Yegneswaran: *Microstructure – property characterization of some Zn-Al alloys: Effects of heat treatment parameters*, Z. Metallkd. 87, 967–972, 1996.
- [20] B. K. Prasad: *Influence of heat treatment parameters on the lubricated sliding wear behavior of a zinc-based alloy*, Wear 257, 1137–1144, 2004.
- [21] S. Murphy, T. Savasakan: *Metallography of Zn-25%Al based alloys in the As-cast and aged conditions*, Practical Metallography 24, 204–221, 1987.
- [22] G. Haorn., T. Xianfa, C. Hongwei, L. Chengdong, Z. Peng: *Antifriction and wear behavior ZAS35 zinc alloy: influence of heat treatment and melting technique*, Materials Science and Engineering 316, 109–114, 2001.
- [23] T. Savaskan, A. Aydiner: *Effects of silicon content on the mechanical and tribological properties of monotectoid-based zinc-silicon-silicon alloys*, Wear 257, 377–388, 2004.
- [24] B. K. Prasad: *Effects of microstructure on the sliding wear performance of Zn-Al-Ni alloy*, Wear 240, 100–112, 2000.
- [25] G. Purcek, Kucukomeroglu, T. Savaskan, S. Murphy: *Dry sliding friction and wear properties of zinc-based alloy*, Wear 252, 894 – 901, 2002.
- [26] M. Babić, R. Ninković, S. Mitrović, I. Bobić: *Influence of heat treatment on tribological behavior of Zn-Al Alloys*, Proceedings of 10<sup>th</sup> International Conference on Tribology, SERBIATRIB '07, Kragujevac, pp. 17–22, 2007.
- [27] M. T. Jovanovic, I. Bobic, B. Djuric, N. Grahovac, N. Ilic: *Microstructural and sliding wear behavior of heat-treated zinc-based alloy*, Tribology letters 25, 173–184, 2007.
- [28] K. H. W. Seah, S. C. Sharma, B. M. Girish: *Mechanical properties of cast ZA-27/graphite particulate composites*, Materials and design, 16, 5, 271–275, 1995.
- [29] R. D. Pruthviraj, P. V. Krupakara: *Influence of SiC additions on mechanical properties of the Zn-Al alloy (ZA-27)*, International Journal of Material Science, Volume 2, Number 1, pp. 53 –57, 2007.
- [30] S.C. Sharma, B.M. Girish, K. Rathnakar, B.M. Satish: *Effect of SiC particle reinforcement on the unlubricated sliding wear behavior of ZA-27 alloy composites*, Wear 213, 33–40, 1997.
- [31] S.C. Tjong, F. Chen: *Wear behaviour of as-cast ZnAl27/SiC particulate Metal-matrix composites under lubricated sliding condition*, Metallurgical and materials transactions A, Vol.28A, September, 1951–1955, 1997.
- [32] I. Bobic, M.T. Jovanovic, N. Ilic: *Microstructure and strength of ZA-27 based composites reinforced with Al<sub>2</sub>O<sub>3</sub> particles*, Materials Letters, 57, 1683–1688, 2003.
- [33] G. Ranganath, S.C. Sharma, M. Krishna: *Dry sliding wear of garnet reinforced zinc/aluminium metal matrix composites*, Wear 251, 1408–1413, 2001.
- [34] S.C. Sharma, B.M. Satish, B.M. Girish, K. Rathnaka, A. Hiroshi: *Dry sliding wear of short glass fibre reinforced zinc-aluminium composites*, Tribology International, Vol. 31, No.4, 183–188, 1998.
- [35] N. Karni, G.B. Barkay, M. Bamberger: *Structure of metal-matrix composite*, Journal of Material science letters, 13, 541–544, 1994.
- [36] S.C. Sharma, B.M. Girish, K. Rathnakar, B.M. Satish: *Sliding wear behavior of zircon particles reinforced ZA-27 alloy composite materials*, Wear 224, 89–94, 1999.
- [37] S.C. Sharma, S. Shanta, M. Krishna: *Effect of aging parameters on the micro structure and properties of ZA-27/aluminate metal matrix composites*, Journal of Alloys and Compounds 346, 292–301, 2002.
- [38] S. Shanta, M. Krishna, U. Jayagopal: *A study on damping behaviour of aluminate particulate, reinforced ZA-27 alloy metal matrix composites*, Journal of Alloys and Compounds 346, 268–274, 2001.
- [39] N. P. Suh, H.C. Sin: *The Genesis of Friction*. Wear 69, 91–114, 1981.
- [40] G. W. Stachowiak, A. W. Batchelor: *Engineering Tribology*, 3rd. ed., Elsevier Butterworth-Heinemann, 2005.